Some Physicochemical Properties of the KOH–H_2O System

Range: 55 to 85 Weight % and 120° to 250° C.

W. M. VOGEL, K. J. ROUTSIS, V. J. KEHRER, D. A. LANDSMAN, and J. G. TSCHINKEL
Physical Chemistry Laboratory, Pratt & Whitney Aircraft, Middletown, Conn. 06458

The binary system, potassium hydroxide–water, was investigated in the range of 55 to 85 weight % of potassium hydroxide and 120 to 250° C. The solid-liquid phase diagram and the density of both phases were established. The other measured properties that were of interest for the application of this system as electrolyte in batteries and fuel cells refer to the liquid state only. Most thoroughly measured was the electrical conductivity as a function of concentration and temperature. Other properties were water pressure, solubility of hydrogen gas, and the transport properties viscosity and diffusivity of water, all measured over most of the quoted range. Potassium hydroxide was of analytical grade. Some values of electrical conductivity and water pressure were also measured with the liquid systems rubidium hydroxide–water and cesium hydroxide–water.

WHEN using KOH–H_2O solution as electrolyte in fuel cells operating at 120° to 250° C., one is forced to maintain the concentration in the range 55 to 85 weight % of KOH to hold the water pressure below about 0.2 atm. to avoid excessive evaporation or the need for pressurizing the cell. Looking for data needed in the calculation of process characteristics one is confronted by a great lack of such data in this range. This prompted the authors to measure the data that are most essential for the fuel cell process. Such data should also be of interest to other industries using this system. The starting material was analytical grade 85% KOH in pellet form. Some measurements were also made on the RbOH–H_2O and CsOH–H_2O system.

PHASE DIAGRAM

A phase diagram covering the entire range of interest here has been published by the Hooker Chemical Co. (*16*) and is reproduced for convenience (Figure 1). Since the branch between the monohydrate (KOH·H_2O) and eutectic, 75 to 85 weight % of KOH, was of particular interest and data from a second source (*4*) were in disagreement, that branch was measured by the authors.

The freezing temperature data were obtained from temperature *vs.* time curves during cooling of about 400 grams of KOH–H_2O contained in a nickel vessel held in a thermostatically controlled bath. The temperature of the bath was lowered at a constant rate; the temperature difference between melt and thermostat was maintained constant at about 5° C. Thus the cooling curve during crystallization became a straight line, permitting precise extrapolation to intersect the straight temperature-time line before the onset of crystallization. This eliminated the error due to undercooling.

Concentrations were determined by titrimetric analysis of a sample withdrawn shortly before the onset of crystallization. The measured data are plotted in Figure 2 and compared with the curves from the other two sources.

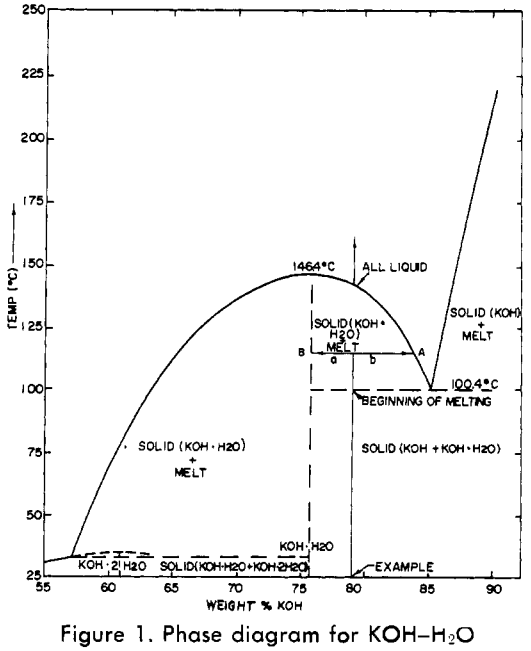

Figure 1. Phase diagram for KOH–H_2O
Source: (*10*)

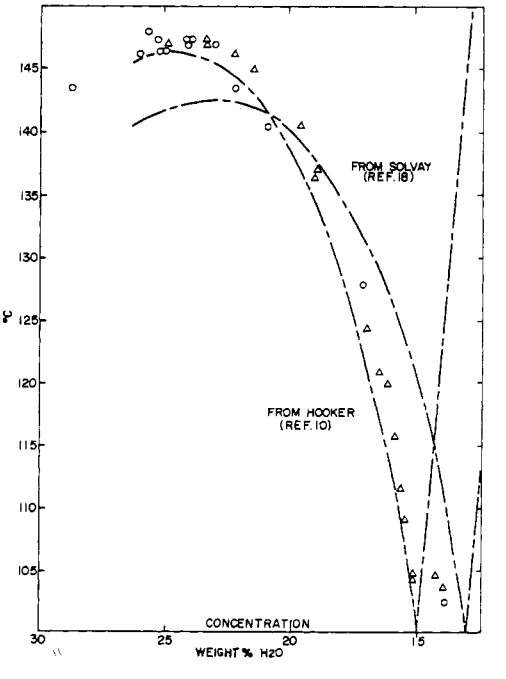

Figure 2. KOH–H_2O (–K_2CO_3) system—freezing temperature *vs.* concentration
○ K_2CO_3/KOH weight ratio = 0.0095
△ Saturated with K_2CO_3 (K_2CO_3/KOH weight ratio = 0.032 ± 0.004)

In some of the present measurements, the carbonate content was 0.8 weight % K_2CO_3 in the commercial pellets (85 weight % KOH); in others K_2CO_3 was made up to saturation by adding a small excess which remained in the solid state.

The K_2CO_3/KOH weight ratio varied over the test range between 0.0095 and 0.032 ± 0.004. No clear trend of solubility with respect to temperature and water content or influence of K_2CO_3 content on freezing temperature could be distinguished.

Most of the author's points fall several degrees above the Hooker curve at the same concentration. Deviation from the Solvay curve is much greater.

DENSITY

Solid State. Gmelin (7) lists d_4^{25} = 2.120 grams per cc. and the cubic expansion coefficient for solid anhydrous KOH:

$$\frac{1}{V_0} \times \frac{dv}{dT} = 1.90 \times 10^{-4}[^\circ C.^{-1}], (30^\circ \rightarrow 130^\circ)$$

which leads to the values:

t, ° C.	25	50	75	95
d_{KOH}, g./cc.	2.120	2.110	2.100	2.092

The solid on the phase diagram (Figure 1) from 75.7 to 100 weight % KOH at T ≤ 100.4° C. was assumed to be a heterogeneous mixture of pure solid KOH and pure solid monohydrate $KOH \cdot H_2O$. The specific volume of any solid made up of these two components is then;

$$v_{KOH-H_2O} = \frac{m_{KOH}}{d_{KOH}} + \frac{m_{KOH \cdot H_2O}}{d_{KOH \cdot H_2O}} = \frac{1}{d_{KOH-H_2O}} \quad (1)$$

where m denotes the mass fraction and $KOH-H_2O$ designates an arbitrary mixture, while $KOH \cdot H_2O$ refers to the monohydrate.

d_{KOH-H_2O} for a solid containing 86 weight % KOH (m_{KOH} = 0.423, $m_{KOH \cdot H_2O}$ = 0.577) was measured. d_{KOH} is given above; putting these data in Equation 1, $d_{KOH \cdot H_2O}$ was calculated for all the temperatures where these data are known.

To test the initial assumption (miscibility of KOH and $KOH \cdot H_2O$ in the solid state), the same procedure was followed for another composition (Table I). If the assumption was correct, the same data for $d_{KOH \cdot H_2O}$ should be obtained. Table II shows good agreement. As the densities for KOH and $KOH \cdot H_2O$ are known, the process can be reversed and the density of any solid mixture between 75.7 and 100 weight % KOH can be calculated at any temperature up to the eutectic temperature (100.4° C.). For convenience, Equation 1 has been rewritten using the total water content instead of the content of pure KOH and the monohydrate $KOH \cdot H_2O$ as in Equation 1:

$$d_{KOH-H_2O,\,solid} = \frac{1}{4.117 \cdot p\left(\frac{1}{d_{KOH \cdot H_2O}} - \frac{1}{d_{KOH}}\right) + \frac{1}{d_{KOH}}} \quad (2)$$

where p = weight fraction H_2O in $KOH-H_2O$. (This equation neglects the presence of K_2CO_3 and assumes that no gas is occluded.)

Liquid Phase. No calculations can be made for the melt. All densities have to be measured. Figure 3 gives data measured according to Archimedes' principle (buoyancy). Accurate data at the higher water contents at high temperatures are difficult to obtain in an open vessel because of the relatively high water vapor pressures.

Within experimental errors, however, both d *vs.* T at constant composition (Figure 3) and a cross-plot of d *vs.* composition at constant temperature are straight lines within the range tested. The error in inter- or extrapolation of these curves will probably be small. The slopes are $\Delta d/\Delta T$ = 0.000714 gram per cc. per deg. and $\Delta d/\Delta$ weight % H_2O = 0.0112 gram per cc. per %.

Two-Phase (Melting) Region. Assuming thermodynamic equilibrium, the density of the solid phase is as given before [below 85.1 weight % KOH (total) the solid phase is $KOH \cdot H_2O$, above that it is KOH].

The over-all density, d (liquid + solid), for the example (Figure 1) at 115.5° C. is then found from

$$\frac{1}{d} = \frac{1}{a+b}\left(\frac{b}{d_{KOH \cdot H_2O}} + \frac{a}{d_{melt}}\right) \quad (3)$$

where a and b are in units of length or weight per cent.

Dihydrate $KOH \cdot 2H_2O$. The $KOH-H_2O$ phase diagram shows a hidden maximum in the melting curve for the dihydrate, $KOH \cdot 2H_2O$. This means that although the solid mixture of $KOH \cdot H_2O$ and $KOH \cdot 2H_2O$ consists of two phases (no solid solutions), no eutectic is formed at 1 atm. pressure because the dihydrate decomposes before it can reach a eutectic. For this reason the pure dihydrate was not prepared, but rather the densities of solid mixtures were measured by the buoyancy of a cylinder in silicon oil. From this density, the density was calculated using the density of $KOH \cdot H_2O$ reported above and correcting for K_2CO_3 and occluded air. The composition of the solid

Table I. Measured Densities for Two Solid $KOH-H_2O$ Mixtures

	Composition, Wt. %			Density, G./Cc. at ° C.			
	KOH	K_2CO_3	H_2O	24	50	75	95
I	86.45	0.68	12.87	2.0055	1.9960	1.9880	1.9820
II	78.7	1.0	20.3	1.9562	1.9450	...	...

Table II. Density of the Monohydrate $KOH \cdot H_2O$ (G./Cc.) Calculated by Equation 1 from Data of Table I

t, ° C.	25	50	75	95
I	1.928	1.920	1.913	1.908
II	1.928	1.916		

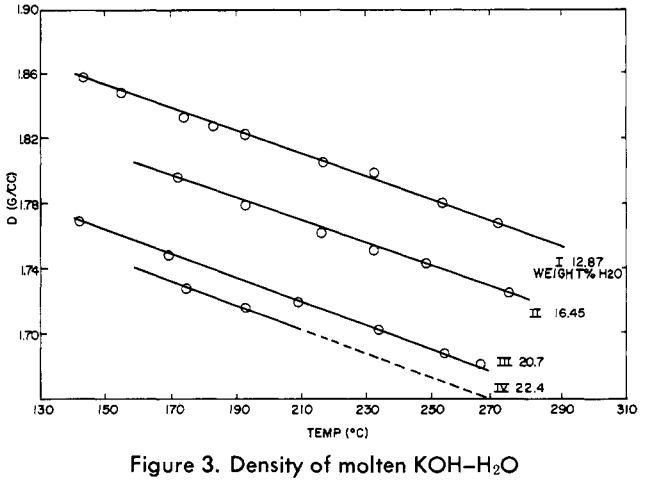

Figure 3. Density of molten $KOH-H_2O$

Accuracy = ±2.2%; $\Delta d/\Delta T = 7.14 \times 10^{-4}$ G./Cc., ° C.

	KOH	K_2CO_3	H_2O
I.	86.45	0.68	12.87
II.	82.70	0.85	16.45
III.	78.26	1.04	20.70
IV.	76.76	0.84	22.40

mixture was obtained from Figure 1. The results for two mixtures are given in Tables III and IV.

Constant-Density Lines of Molten KOH–H_2O. Using all the data measured and calculated so far, a diagram of lines of constant density in concentration-temperature coordinates was designed (Figure 4). The densities in the two-phase regions are calculated. The precision depends on that of the densities of the single phases and the accuracy of the phase diagram. This means that in areas well inside two-phase regions the precision in d is similar to that for the single phases, ± 2 to 3%. For compositions close to the borders of the two-phase regions, however, the error may rise steeply, reaching the highest values in the vicinity of the maximum and can reach the full difference of the densities of solid and liquid, approximately 10%.

Aqueous KOH Solutions. To fill the gap between the author's data on the molten system and the data of Akerlof and Bender (*1*) in the range 0 to 50 weight % KOH, four isotherms were measured between 140° and 185° C. and 50 to 75 weight % KOH by the buoyancy method. The four isotherms had slopes of Δd/weight % KOH = 0.0113 gram per cc., per % KOH with an average deviation of 0.0001. The spread of data of the isotherms was no greater than ± 0.3%. From these isotherms, lines of constant concentration in coordinates of density *vs.* temperature were derived as in Figure 5.

WATER PRESSURE OVER MOLTEN ALKALI HYDROXIDE–H_2O SYSTEMS

Data on NaOH–H_2O and KOH–H_2O in the molten range were published by Merkel (*18*). For the present measurements a thermogravimetric method was used: a sample suspended on a recording balance was exposed at a fixed temperature to a H_2O–N_2 mixture of controlled composition. When equilibrium (constant weight) was reached, the composition was determined from the weight and titration of the sample.

Such data over the range 60 to 80 weight % KOH and 140° to 200° C. are shown in Figure 6; the curves also show the small increase of p_{H_2O} when the K_2CO_3 content is raised from 0.89 weight % (commercial) to saturation (approximately known as more than 2.5 but less than 5 weight %).

The equilibrium compositions of the sodium, potassium, rubidium, and cesium hydroxides at p_{H_2O} = 1 atm. were measured as a function of temperature (Figure 7). On the basis of equal molar concentration, it shows the water fugacity to be lowest for KOH, followed by RbOH, CsOH, and NaOH; in other words, at equal p_{H_2O}, KOH solutions have the lowest molarity in KOH (retain water most tenaciously).

Table III. Composition of Mixtures Measured

Mixt.	KOH, %	H_2O, %	K_2CO_3, %	KOH·H_2O, %	KOH·$2H_2O$, %
a	61.14	37.66	1.20	6.52	92.26
b	61.98	36.34	1.68	14.22	84.10

Table IV. Calculation of Density of Dihydrate KOH·$2H_2O$

Mixt.	T, ° C.	d, Measured	d, K_2CO_3	d, KOH·H_2O	d, KOH·$2H_2O$
a	+2	1.648	2.43	1.934	1.638
	21	1.640	2.43	1.929	1.616
	24	1.66	2.43	1.926	1.65
b	−9	1.702	2.43	1.937	1.658
	0	1.703	2.43	1.935	1.659
	25	1.67	2.43	1.926	1.62

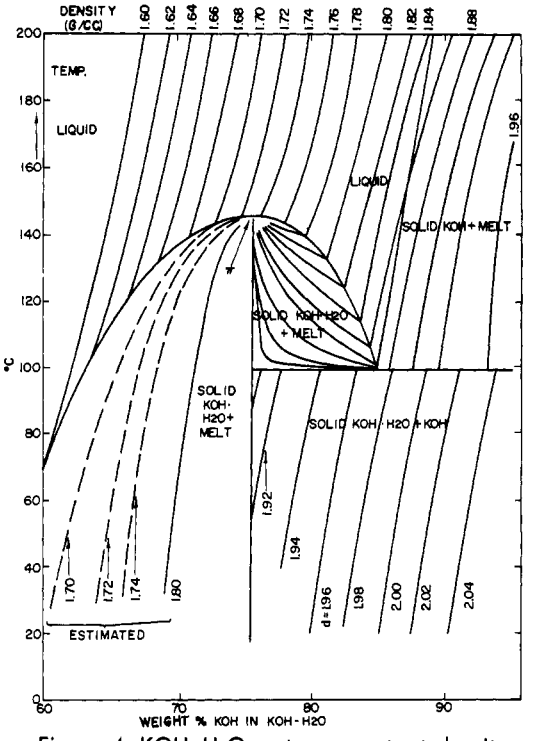

Figure 4. KOH–H_2O system: constant density lines in temperature *vs.* concentration coordinates

π = Singularity point—i.e., it is not possible to reach this point without density changes

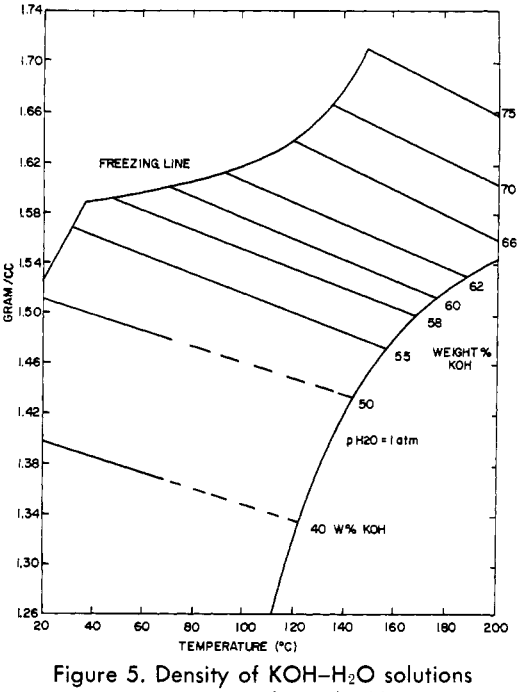

Figure 5. Density of KOH–H_2O solutions *vs.* temperature and weight % water

The equilibrium composition of RbOH–H_2O at various water pressures (0.17 to 0.48 atm.) and temperatures (130° to 190° C.) was measured, and data were plotted as constant composition curves (Figure 8).

SOLUBILITY OF H_2 IN MOLTEN KOH–H_2O

The method is based on saturating the melt with H_2, followed by an argon sweep and gas chromatography of the sweep gas for H_2.

About 500 ml. of molten KOH–H_2O was contained in a nickel flask (I) connected to a second similar flask (II).

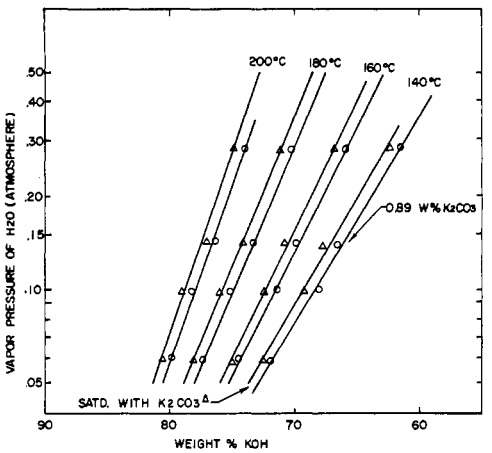

Figure 6. Water vapor pressure over molten KOH–K_2CO_3–H_2O

O = 0.89 weight % K_2CO_3

△ = Saturated with K_2CO_3

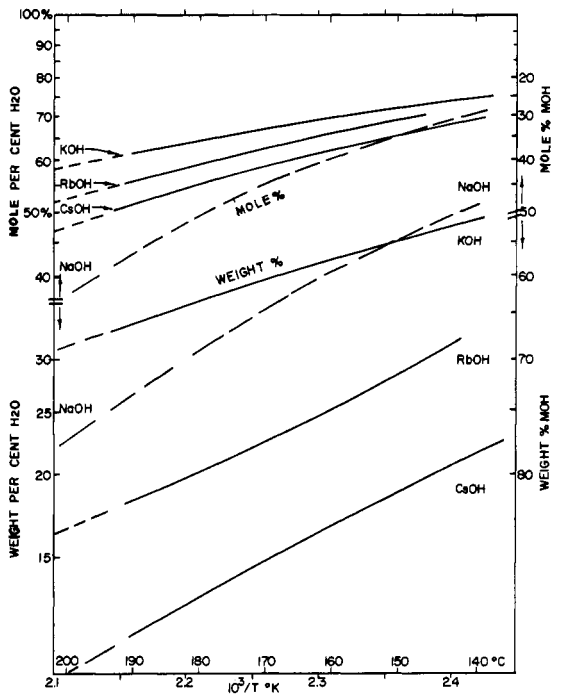

Figure 7. Equilibrium compositions of alkali hydroxide–water at 1 atm. water pressure

CsOH:
RbOH: } Measured at PWA
KOH:

NaOH: Bulletin of U. S. Ind. Chem. Corp. on caustic soda

The melt was saturated with H_2 through a nickel frit, after which a rest period allowed the rise of suspended gas bubbles; then the melt was transferred from vessel I into vessel II (which had been swept by argon) by applying H_2 pressure to vessel I. An electrolytic level probe assured that the level of liquid did not drop below the outlet near the bottom of vessel I, so that no H_2 gas could be transferred to vessel II. Then the melt in vessel II was swept by argon, the sweep gas collected, measured (about 3 liters), and chromatographed for its H_2 content.

Two sets of data, taken at 1 atm. total pressure (p_{H_2} + p_{H_2O}), are given in Figure 9. The correction of p_{H_2} = 1 atm. is based on Henry's law.

Plotting the data of Knaster and Apelbaum (*15*) at 75° C. and the author's data at 200° C., on the same coordinates (Figure 9) shows that, at the lower temperature and concentration, the solubility of H_2 decreases with increasing KOH

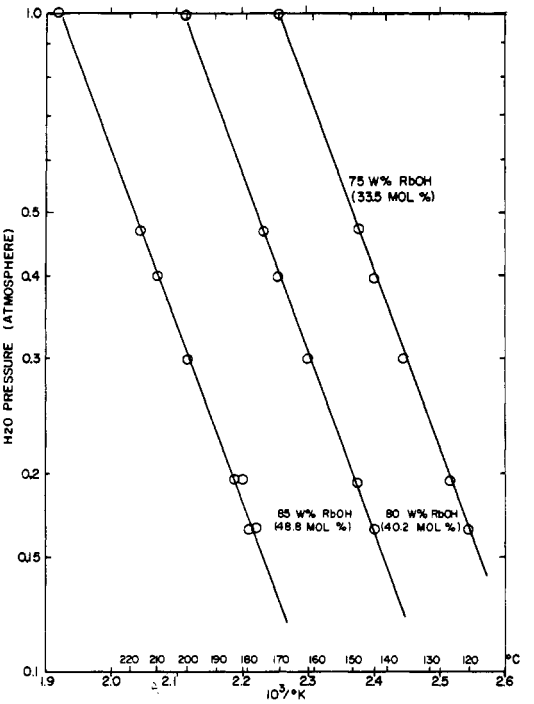

Figure 8. Water pressure of RbOH–H_2O *vs.* temperature at fixed composition

Composition of anhydrous substrate

	Weight %	Mole %
RbOH	92.3	96.5
Rb_2CO_3	7.7	3.5

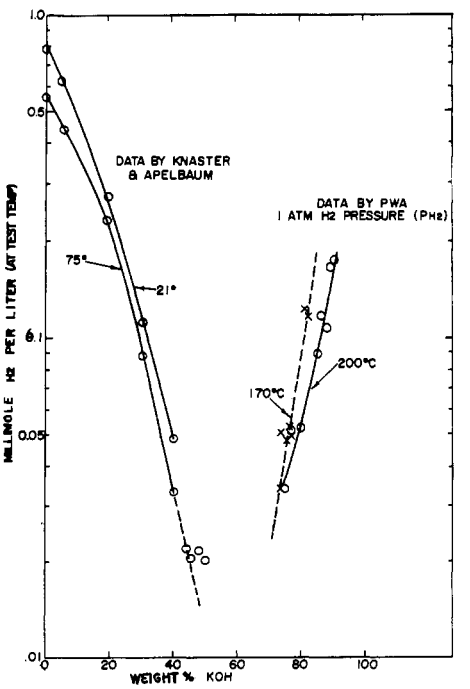

Figure 9. Comparison of two regions of solubility of H_2 in KOH–H_2O

concentration as is normal for an aqueous solution, whereas at the higher temperature and concentration the reverse is true. Somewhere between these two conditions there must be a reversal of the trend. This is of considerable theoretical and practical interest, but unfortunately it was not possible to measure in that range at atmospheric pressure. A pressurized apparatus would be needed.

ELECTRIC CONDUCTIVITY

Experimental. Electrolyte resistances were determined by the four-electrode method. Previously reversible electrodes were used as probes (*6, 12, 13*). But results are satisfactory if the potentials of the probes remain constant during an experiment without being truly reversible. Small wires polarized by constant anodic current were used as probes. The drift in the difference of the potentials of two such probes was not more than 1 to 2 mv. over periods of 10 minutes or more. The time required to impose a measuring current, and to measure the resulting change in the potential difference between probes was not more than 5 to 10 seconds. By keeping the currents polarizing the probes small compared with the measuring current and by widely separating the paths of these currents (Figure 10), polarized electrodes were satisfactory probes in the four-electrode method.

The cell was machined from Teflon TFE (Figure 10). All four-electrodes were made of 80% Au-20% Pd (*17*).

The galvanostatic circuit for polarizing the probes consisted of $5M$ resistors and 45 volt dry batteries. The whole circuit is given in Figure 11.

The cell constant, K, was determined by measuring the resistance of the cell filled with 0.1 and $1N$ KCl at 25° C. Specific conductivities for these solutions were taken from Conway (*5*). Within experimental error, K determined for both solutions and calculated from the cell dimension agreed. K for higher temperatures was calculated from $K^{25°\,C.}$ using the value of

$$\alpha = 1.7 \times 10^{-4}[\text{deg.}^{-1}]$$

for the expansion coefficient of Teflon. The reversibility of the Teflon expansion was checked by frequently redetermining K. K changed from 399 to 386 cm.$^{-1}$ during the initial 15 hours of operation, then to 377 cm.$^{-1}$ over the next 6 months.

The electrolyte was prepared with doubly distilled water and reagent grade KOH without further purification. Samples, taken after each experiment, were analyzed for KOH and K_2CO_3 by titrating with HCl against phenolphthalein and bromocresol green–methyl red as indicators.

One difficulty encountered was the formation of gas bubbles inside the cell capillaries. Below 220° C., these bubbles were removed immediately before each measurement by sweeping with a Teflon-coated rod. At temperatures above 220° C., no satisfactory measurements were possible, since bubbles formed too rapidly, owing to rapid attack of the Teflon by KOH under formation of H_2.

Results. KOH–H_2O. The resistances of a particular electrolyte were always measured in one run as a function of temperature.

No influence of variations in carbonate content (1 to 2 weight %) on the conductivity could be found. All data fitted closely the form

$$\log \kappa = A - B/T \qquad (4)$$

From such plots, data at 10° C. intervals were interpolated. No interpolation exceeded 5° C. No extrapolations were made. The results are given in Figure 12.

The experimental reproducibility was ±1.5%. The estimated sum of errors from all sources is ±3.5%.

These data agree closely with those by Klochko and Godiva (*14*) for 150° and 175° C. At lower temperature, discrepancies between the present data and theirs exist.

RbOH–H_2O, CsOH–H_2O. Conductivities of these systems were determined at three concentrations and for the range 150° to 225° C. (Figures 13 and 14).

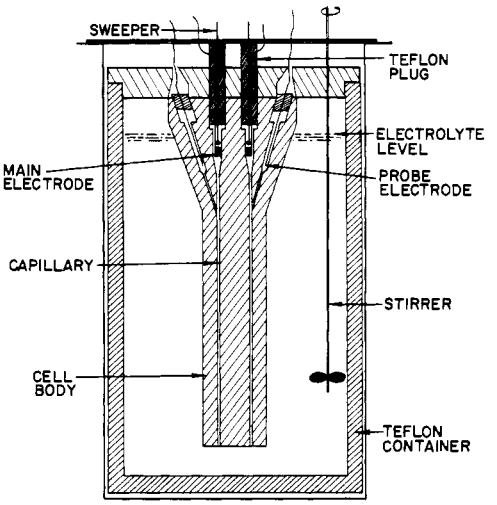

Figure 10. Cell for measuring the electric conductivity of molten alkali hydroxides

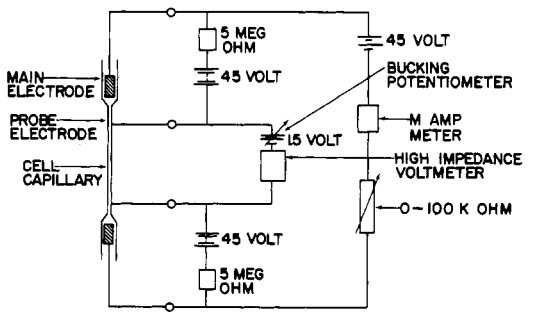

Figure 11. Circuit for measuring electric conductivity by DC-method

VISCOSITY OF KOH–H_2O SOLUTIONS

A rolling ball viscometer (*11*) was used to determine the viscosities of KOH–H_2O solutions at atmospheric pressure over the liquid range (0- to 70-mole % KOH and 10° to 240° C.).

The viscometer was constructed from a 30-inch length of 0.4-inch diameter nickel tube with flanged ends. The tube was wound noninductively with insulated heating tape and was supported at its midpoint in such a way that

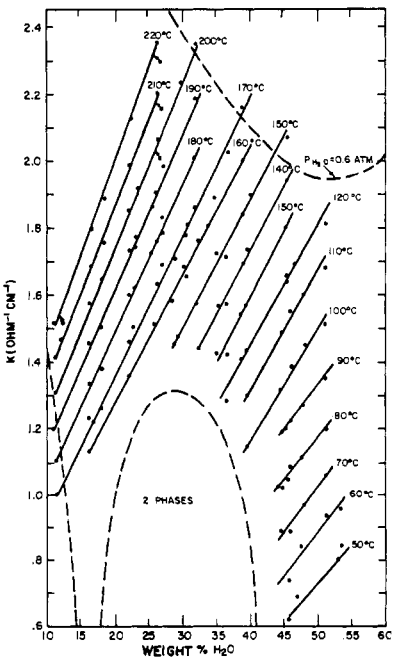

Figure 12. Electric conductivity of molten KOH–H_2O

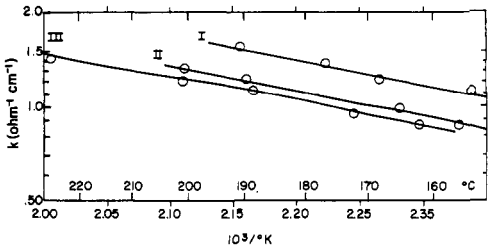

Figure 13. Electric conductivity of molten rubidium hydroxide–water

Composition in weight %

	I	II	III
RbOH	78.09	83.55	85.11
Rb_2CO_3	2.84	2.91	3.43
H_2O	19.07	13.54	11.46
Mole % H_2O	57.8	47.6	42.9

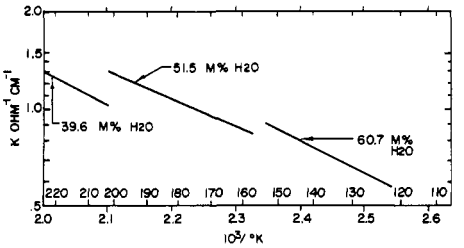

Figure 14. Electrical conductivity of cesium hydroxide–H_2O systems

Composition in weight %

	I	II	III
CsOH	87.0	85.2	79.9
Cs_2CO_3	5.7	3.5	4.5
H_2O	7.3	11.3	15.6
Mole % H_2O	39.6	51.5	60.7

it could be tilted freely in a vertical plane to $\pm 10°$ from the horizontal. Inside the tube was a gold-plated $\frac{3}{8}$-inch diameter (Type 316) stainless steel ball. The ends of the tube were sealed by flanged plates bearing thermocouple wells and sensing devices to detect the arrival of the ball. The solutions were admitted to the tube under vacuum through a vertical side arm attached near one end, which also served as an expansion chamber and bubble trap.

From the known viscosities (η) of calibrating solutions (*2*)—water-ethanol and water-sucrose—and the measured time taken for the ball to roll down the tube, constants A and B in Equation 5 were evaluated:

$$\eta = A \cdot t(\Delta\rho) + B \tag{5}$$

where $\Delta\rho$ is the difference between the density of the ball and that of the solution through which it passes, and t is the time taken for the ball to roll down the tube when the tube is tilted to a preset angle from the horizontal.

Viscosity-composition isotherms derived from measurement in which the tube contained KOH–H_2O solutions at various temperatures are shown in Figure 15, with values taken from the literature (*9, 10*).

DIFFUSIVITY OF H_2O IN MOLTEN KOH–H_2O

The method of diffusion between a large bulk of concentration, C_0, and narrow capillaries filled with initial concentration, C_1, was chosen (*3, 8*). Ten capillary tubes made from nickel, 0.124-cm. I.D., 4 cm. long, were inserted vertically, open end up, into a nickel disk about 5 cm. away from a supporting shaft which rotates the whole assembly submerged in about 500 ml. of bulk solution held in a nickel pot.

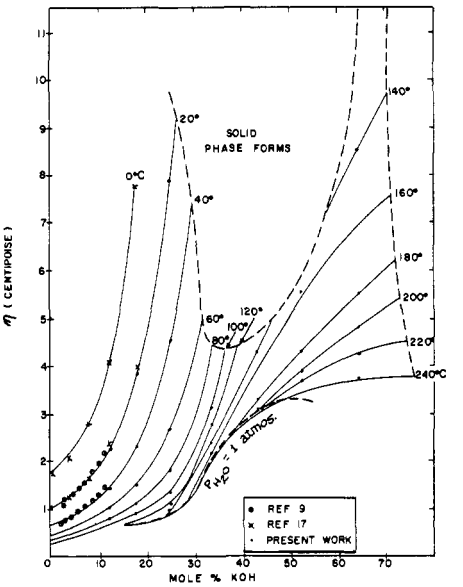

Figure 15. Viscosity of molten KOH–H_2O

Isotherms vs. mole % KOH

Complete filling of the capillaries was ensured by submerging them in a separate vessel under a melt of concentration C_1 and evacuating.

The filled capillaries were introduced into the test vessel where they were allowed to come to temperature (about 5 minutes before being submerged in the KOH–H_2O bulk melt (higher water concentration, C_0). The capillary holding disk was rotated about 6 r.p.m. Every 5 to 10 hours, two capillaries were withdrawn and their average KOH concentration was determined by titration.

$$\frac{\bar{C} - C_1}{C_0 - C_1} = \frac{2}{l}\left[\frac{Dt}{\pi}\right]^{1/2} \tag{6}$$

where

$\bar{C}$ = final average concentration of H_2O in capillary
C_1 = initial concentration of H_2O in capillary
C_0 = concentration of H_2O in bulk
l = length of capillary (inside), cm.
t = time, sec.
D = diffusivity of H_2O, sq. cm./sec.

The fractional concentration difference *vs.* $(\text{time})^{1/2}$ plotted as a straight line as long as the concentration change had not reached the bottom of the capillaries.

Table V. Diffusivity of H_2O in KOH–H_2O at 227 °C.

Capillary No.	4		5		6	
	t, hr.	Sq. cm. $\text{sec.}^{-1} \times 10^4$	t, hr.	Sq. cm. $\text{sec.}^{-1} \times 10^4$	t, hr.	Sq. cm. $\text{sec.}^{-1} \times 10^4$
1	2	1.81	2	...	4	...
2	2	0.88	2	1.33	4	1.22
3	4	1.22	4	2.14	4	1.20
4	4	1.19	4	1.54	4	1.27
5	8	1.34	6	1.51	4	1.34
6	8	1.49	6	1.73	8	1.36
7	12	1.27	10	1.96	8	1.46
8	12	1.72	10	1.45	8	1.28
9	23.3	1.08	20	1.18	8	1.23
10	23.3	1.22	20	1.24	8	1.23

Table VI. Dependence of Diffusivity of H_2O in KOH–H_2O Melt on Temperature

Run No.	No. of Capill.	Temp., °C.	C_1, % H_2O	C_0, % H_2O	$C_0 - C_1$, % H_2O	$(C_0 + C_1)/2$, % H_2O	$D \times 10^4$ Sq. Cm. Sec.$^{-1}$ Av. per run	Av. for each temp.
2	6	227	13.38	20.78	7.40	17.08	1.41	
4	8	227	12.90	22.00	9.10	17.45	1.32	
5	7	227	13.21	21.63	8.42	17.42	1.43	
6	9	227	13.47	21.79	8.32	17.63	1.29	1.31
18	10	225	15.01	23.78	8.77	19.40	1.201	
7	8	203	17.23	22.16	4.93	19.70	1.13	
17	8	202	14.59	24.14	9.55	19.36	1.147	1.14
10	9	176	17.41	22.33	4.92	19.87	0.710	
11	8	176	17.63	22.22	4.59	19.93	1.025	
12	7	176	13.70	22.30	8.60	18.00	0.727	0.789
16	6 & 6	176	14.79	24.37	9.58	19.57	0.751	
							0.701	
8	6	151	17.38	22.21	4.83	19.79	0.616	
9	7	151	17.42	22.34	4.92	19.88	0.604	
15	8	152	14.40	24.32	9.92	19.46	0.698	0.643
	n = 113							

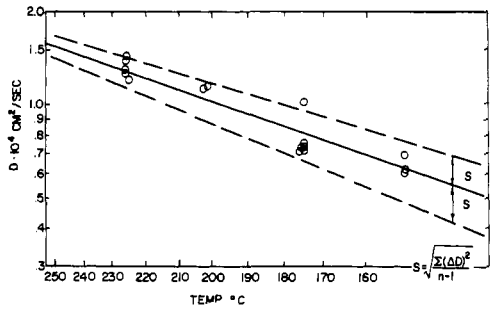

Figure 16. Diffusivity of H_2O in KOH–H_2O as a function of temperature

Median H_2O concentration approx. 20 weight % H_2O

Each point is the average from 5 to 10 capillaries

The reproducibility of filling the capillaries and analyzing their content was determined by filling and analyzing 10 of them (no diffusion). The water content was 13.75 weight % average, the average error of the mean: $\Sigma\ (\Delta x)/n\ (n)^{1/2} = 0.06$ weight %, where Δs is deviation from average, and n is number of measurements.

Three runs were made at 227° C. with 10 capillaries each; capillaries were withdrawn in groups of two to five at intervals of 2 to 23 hours. Table V shows the values of D calculated by Equation 6. The value of $D_{227°\,C.} = 1.38 \times 10^{-4}$ sq. cm. per sec. (80% KOH median concentration) appears to be of low random error but could still contain a systematic error.

D (Sq. cm. per sec.) = $1.38\ (\pm 0.04) \times 10^{-4}$

Av. error of mean = $\Sigma\ (\Delta D)/n\ (n)^{1/2} = 0.038$

Temperature Dependence. The temperature was varied from 150° to 230° C. at a median concentration of about 200 weight % H_2O (80% KOH). Table VI indicates the number of runs, each for six to 10 capillaries removed at intervals of 2 to 12 hours.

The fractional concentration change for each capillary of the same run was plotted *vs.* time and the diffusivity value calculated (Table VI and Figure 16). The straight line was calculated by the least squares method:

$$\log D_{(80\%\ KOH)} = \frac{914.5}{T\ (°\,K)} - 2.0464 \text{ (sq. cm. per sec.)} \qquad (7)$$

The standard error is

$$S = \left(\frac{\Sigma\ (\Delta D)^2}{n-1}\right)^{1/2} = 0.142 \times 10^{-4} \text{ sq. cm. per sec.}$$

Concentration Dependence. The authors attempted to obtain the concentration dependence of diffusivity at a fixed temperature of 150° C. Data were evaluated from seven runs of about 10 capillaries each covering a range of average water concentration from about 15 to 30 weight % (Table VII).

The data for all single capillaries were plotted and a least square fitted line was calculated (Figure 17). The scatter of data was much greater at higher dilution (above 30% H_2O), so such data had to be discarded.

Table VII. Dependence of Diffusivity of H_2O in KOH–H_2O Melt at 151 ± 2° C. on the Mean H_2O Concentration

Run No.	No. of Capill.	C_1, % H_2O	C_0, % H_2O	$C_0 - C_1$, % H_2O	$(C_0 + C_1)/2$, % H_2O	$D \times 10^4$ Sq. Cm. Sec.$^{-1}$ Av. per Run
21	10	12.83	19.58	6.75	16.21	0.573
15	9	14.40	24.32	9.92	19.46	0.698
8	6	17.38	22.21	4.83	19.79	0.616
9	7	17.42	22.34	4.92	19.88	0.604
19	10	24.56	32.78	8.22	28.67	0.779
13	10	24.81	33.74	8.93	29.28	0.943
20	7	29.32	35.19	5.87	32.26	0.937

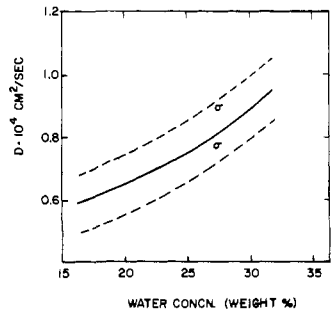

Figure 17. Diffusion of H_2O in KOH–H_2O melt

$D \times 10^4$ *vs.* water concn. (weight %)

Temperature 151° ± 2° C.

$\sigma = [(\Delta D)^2/n - 1]^{1/2}$

$\sigma = 0.10 \times 10^{-4}$ sq. cm. per sec.

LITERATURE CITED

(1) Akerlof, G., Bender, P., *J. Am. Chem. Soc.* **63**, 1088 (1941).
(2) Bingham, E.C., Jackson, R.F., *Natl. Bur. Std. Bull.* **14**, 59 (1918).
(3) Bockris, J.O'M., White, J.L., MacKenzie, J.D., "Physico-Chemical Measurements at High Temperature," p. 306 ff., Butterworths, London, 1959.
(4) Cohen-Adad, R., Michaud, M., *Compt. Rend.* **242**, 2569–71 (1956).
(5) Conway, B.E., "Electrochemical Data," Elsevier, New York, 1952.
(6) Elias, L., Schiff, H.I., *J. Phys. Chem.* **60**, 595 (1956).
(7) "Gmelin's Handbuch der Anorg. Chemie," 8th ed. (No. 1), p. 212 (1936).
(8) Grace, R.E., Derge, G., *Trans. AIME.* **203**, 839 (1955).

(9) Hitchcock, L.B., McIlhenney, J.S., *Ind. Eng. Chem.* **27**, 461 (1935).
(10) Hooker Electrochemical Co., New York, Nalk Bulletin, 1955.
(11) Hubbard, R.B., Brown, G.G., *Ind. Eng. Chem., Anal. Ed.* **15**, 212 (1943).
(12) Ives, D.J., Swaroopa, S., *Trans. Faraday Soc.* **49**, 788 (1953).
(13) Jerris, R.E., Muir, D.R., Gordon, A.R., *J. Am. Chem. Soc.* **75**, 2855 (1953).
(14) Klochko, M.A., Godiva, M.M., *Russ. J. Inorg. Chem.* **4**, 964 (1959).
(15) Knaster, M.B., Apelbaum, L.A., *Zh. Fiz. Khim.* **38**, (1), 223–5 (1964).
(16) Lang, E., Hooker Chemical Co., November 1949.
(17) Lorenz, M.R., Ph.D. dissertation, Rensselaer Polytechnic Institute, Troy, N. Y., 1960.
(18) Merkel, F., *Z. Ver. Deut. Ing.* **72**, 113 (1928).

RECEIVED for review June 23, 1966. Accepted July 20, 1967.

Densities and Molar Volumes of Binary Solutions of Nitroparaffins in Carbon Tetrachloride

CLAUDE R. GUNTER, JOHN F. WETTAW, JERRY D. DRENNAN, RICHARD L. MOTLEY, MICHAEL L. COALE, THOMAS E. HANSON, and BORIS MUSULIN
Department of Chemistry, Southern Illinois University, Carbondale, Ill. 62901

The densities of binary solutions of nitromethane in carbon tetrachloride and nitroethane in carbon tetrachloride were measured at 30°, 35°, and 45° C. The molar volumes and excess molar volumes of mixing were calculated from the observed densities. The data indicated that a single specie of nitroparaffin exists in such binary solutions.

IN RECENT years (*4*), suggestions have been made that nitromethane is a dimer and that solutions of nitromethane in carbon tetrachloride contain equilibrium mixtures of monomer and dimer. The purpose of this investigation was to ascertain whether solutions of either nitromethane or nitroethane in carbon tetrachloride appear to be regular or whether they exhibit wide deviations from regularity. The method used was the determination of density (or a function of density) as a function of concentration. Also, temperature effects were investigated.

EXPERIMENTAL

Specific gravities were taken in a 25-ml. Gay-Lussac pycnometer, Type B bottle (Scientific Glass Apparatus Co., Inc.), using the method described by Weissberger (*12*) and refined by Van Lente (*11*). Weighings (a minimum of three) were made with Christian Becker, Class S, uncalibrated weights. Fisher certified grades of carbon tetrachloride and nitromethane, high purity research samples of nitromethane and nitroethane (Commercial Solvents), and highest purity nitroethane (Brothers Chemical Co.) were used without further purification. No attempt was made to exclude air from the reference liquid (distilled water). The solutions were prepared by mixing volumes of pure components. The estimated cumulative transfer error was ±0.005 mole fraction. Temperatures were regulated (±0.02° C.) by a Precision Scientific Co. bath (No. 66580) and Merc to Merc Model PS-62510-D1 thermoregulator. Temperature readings, precise to ±0.01° C., were obtained with a thermometer calibrated with a National Bureau of Standards thermometer. The precision in the weight readings dictated rounding of the temperature readings (by 0.1° C. or less) to integral values. All calculations were performed on an IBM 1620 computer with 40K storage using an IBM PR 025 monitor with programs written in Fortran II.

RESULTS

Two independent sets of measurements were made at the lowest temperature in order to determine the effect of personal error. This error proved to be of the same order of magnitude as the errors in individual precision. Consequently, only one set of measurements was made at other temperatures. Readings were either corrected to vacuo or discarded if their deviations obeyed a standard discard criterion (*7*). In the case of a suspect result, the final density value was obtained as a weighted average of independent measurements. The final results are given in Table I.

Individual probable errors (*3*) and, where necessary, weighted probable errors were determined for each density. Insomuch as the probable error only indicates wherein 50% of the readings may lie, an average error based upon weight readings appeared to be more indicative of the precision within the individual experiment. An average error was derived from the definition of the specific gravity, d_t^t,

$$d_t^t = \frac{A \pm a}{B \pm b} \tag{1}$$

where A and B are two weight readings with errors a and b, respectively. After expansion of the denominator, a subsequent multiplication yields the series equation

$$d_t^t = \frac{A}{B} \pm \frac{a}{B} \mp \frac{Ab}{B^2} - \frac{ab}{B^2} + \ldots \tag{2}$$

Since the error terms containing $1/B^2$ are of second order compared with the error term containing $1/B$, the average error was taken to be a/B and is given in Table I. With two exceptions, the maximum average error was 0.0002